

Nambu–Jona-Lasinio-based study of the QCD critical line

A. Barducci,^{*} R. Casalbuoni,[†] G. Pettini,[‡] and L. Ravagli[§]

Department of Physics, University of Florence

and INFN Sezione di Firenze, Via G. Sansone 1, I-50109, Sesto Fiorentino, Firenze, Italy

(Received 11 August 2005; published 21 September 2005)

We employ a 3 flavor Nambu–Jona-Lasinio (NJL) model to stress some general remarks about the QCD critical line. The dependence of the critical curve on $\mu_q = (\mu_u + \mu_d)/2$ and $\mu_I = (\mu_u - \mu_d)/2$ is discussed. The quark masses are varied to confirm that, in agreement with universality arguments, the order of transition depends on the number of active flavors N_f . The slope of the critical curve vs chemical potential is studied as a function of N_f . We compare our results with those recently obtained in lattice simulations to establish a comparison among different models.

DOI: [10.1103/PhysRevD.72.056002](https://doi.org/10.1103/PhysRevD.72.056002)

PACS numbers: 11.10.Wx, 12.38.–t, 25.75.Nq

I. INTRODUCTION

In recent years, the study of the QCD phase diagram by means of numerical lattice simulations has improved considerably. In particular, the presence of a critical ending point, first discovered within microscopical effective models [1–3], appears to be a solid feature [4,5], although its exact location along the critical curve is still controversial. Moreover, the incoming realization of LHC enhances the interest of the scientific community in this kind of problem. The main problem regarding the lattice study of QCD phase diagram is related to the so called sign problem; the fermionic determinant is not positive definite at finite baryon chemical potential, and therefore, to avoid this unwelcome feature, some suitable tricks are needed. The most commonly used between them are the study of QCD at imaginary chemical potential [6–8], the reweighting procedure [4] and Taylor expansion in μ/T [9,10]. A possible way of avoiding the sign problem is to consider QCD at finite isospin chemical potential μ_I : in this case, the fermion determinant is real and positive definite, and standard Monte Carlo simulations are allowed [11,12]. Furthermore, the regime of finite μ_I can be also studied within a class of effective models, and the results can be compared with those obtained on the lattice in order to check the consistency of different approaches. Two properties are remarkable and are of interest at $\mu_I \neq 0$: pion condensation and the splitting of critical curves related with light flavors. The former has been the subject of several studies within different models, starting from effective Lagrangians [13,14], random matrices [15], Nambu–Jona-Lasinio (NJL) [16,17] and ladder-QCD [18] and so apparently a model-independent phenomenon. However, pion (and kaon [19]) condensation would not be accessible from heavy ion experiments, but could regard the physics of compact stars. The latter question is slightly

more controversial: the role played by instantons seems to be crucial to determine whether values of μ_I obtainable in experiments can produce the separation of critical lines [20]. The aim of this paper is to offer an overview of results concerning the behavior of the critical line, obtained in the NJL model and directly comparable with recent lattice analyses. In its strong simplicity, the NJL model recovers the basic structure of nonperturbative dynamics ruling the problem. Therefore, it can be trusted as a good toy model for the study of QCD phase diagram.

II. THE MODEL

Let us now consider the Lagrangian of the NJL model with three flavors u, d, s , with current masses $m_u = m_d = m$ and m_s and chemical potentials μ_u, μ_d, μ_s respectively

$$\begin{aligned} \mathcal{L} &= \mathcal{L}_0 + \mathcal{L}_m + \mathcal{L}_\mu + \mathcal{L}_4 + \mathcal{L}_6 \\ &= \bar{\Psi} i \hat{\partial} \Psi - \bar{\Psi} \underline{\mathcal{M}} \Psi + \Psi^\dagger \underline{\mathcal{A}} \Psi + G \sum_{a=0}^8 [(\bar{\Psi} \lambda_a \Psi)^2 \\ &\quad + (\bar{\Psi} i \gamma_5 \lambda_a \Psi)^2] + K [\det \bar{\Psi} (1 + \gamma_5) \Psi \\ &\quad + \det \bar{\Psi} (1 - \gamma_5) \Psi], \end{aligned} \quad (1)$$

where

$$\begin{aligned} \Psi &= \begin{pmatrix} u \\ d \\ s \end{pmatrix}, \quad \underline{\mathcal{A}} = \begin{pmatrix} \mu_u & 0 & 0 \\ 0 & \mu_d & 0 \\ 0 & 0 & \mu_s \end{pmatrix}, \\ \underline{\mathcal{M}} &= \begin{pmatrix} m & 0 & 0 \\ 0 & m & 0 \\ 0 & 0 & m_s \end{pmatrix}. \end{aligned} \quad (2)$$

$\underline{\mathcal{M}}$ is the current quark mass matrix which is taken diagonal and $\underline{\mathcal{A}}$ is the matrix of the quark chemical potentials. As usual $\lambda_0 = \sqrt{3} \mathbf{I}$ and $\lambda_a, a = 1, \dots, 8$ are the Gell-Mann matrices.

The 't Hooft determinant term, for the three flavors case, corresponds to a six fermion interaction. By working at the mean-field level, the six fermion term can be recast into an effective four-fermion one. In such a way the Lagrangian

^{*}Electronic address: barducci@fi.infn.it

[†]Electronic address: casalbuoni@fi.infn.it

[‡]Electronic address: pettini@fi.infn.it

[§]Electronic address: ravagli@fi.infn.it

(1) reduces to the usual NJL Lagrangian, apart from a redefinition of the four-fermion coupling constant G into a new set of effective ones, taking into account the flavor mixing arising from the 't Hooft term [21,22]

Therefore, because we are dealing with four-fermion interactions only, we can calculate the effective potential by using the standard technique to introduce bosonic (collective) variables through the Hubbard-Stratonovich transformation and by integrating out the fermion fields in the generating functional. If we limit ourselves to consider the

three scalar condensates, and the pseudoscalar condensate in the light quark sector only, the one-loop effective potential we get is

$$V = \frac{\Lambda^2}{8G}(\chi_u^2 + \chi_d^2 + \chi_s^2) - \Lambda^3 \frac{K}{16G^3} \chi_u \chi_d \chi_s + \frac{\Lambda^2}{4G} \left(1 - \frac{K\Lambda\chi_s}{8G^2}\right) (\rho_{ud}^2) + V_{\log}, \quad (3)$$

where

$$V_{\log} = -\frac{1}{\beta} \sum_{n=-\infty}^{n=+\infty} \int \frac{d^3 p}{(2\pi)^3} \text{Tr} \log \begin{pmatrix} h_u & -\gamma_5 \Lambda \rho_{ud} \left(1 - \frac{K\Lambda\chi_s}{8G^2}\right) & 0 \\ \gamma_5 \Lambda \rho_{ud} \left(1 - \frac{K\Lambda\chi_s}{8G^2}\right) & h_d & 0 \\ 0 & 0 & h_s \end{pmatrix}, \quad (4)$$

$$h_f = (i\omega_n + \mu_f)\gamma_0 - \vec{p} \cdot \vec{\gamma} - M_f.$$

In Eq. (4) Tr means trace over Dirac, flavor and color indices and $\omega_n = (2n+1)\pi/\beta$ are the Matsubara frequencies. The dimensionless fields χ_f and ρ_{ud} are connected to the scalar and pseudoscalar condensates, respectively, by the following relations

$$\chi_f = -4G \frac{\langle \bar{\Psi}_f \Psi_f \rangle}{\Lambda}, \quad \rho_{ud} = -2G \frac{\langle \bar{u} \gamma_5 d - \bar{d} \gamma_5 u \rangle}{\Lambda}, \quad (5)$$

and are variationally determined at the absolute minimum of the effective potential. The constituent quark masses are

$$M_i = m_i + \Lambda \chi_i - \Lambda^2 \frac{K}{G^2} \frac{\chi_j \chi_k}{8} (i \neq j \neq k). \quad (6)$$

Since the model is nonrenormalizable, we have to introduce the hard cutoff Λ on the three-momentum.

Through this article we consider the physical case (with realistic values of meson masses and decay constant), we assume for the parameters the same values as in Ref. [22]

$$\Lambda = 631.4 \text{ MeV}, \quad G\Lambda^2 = 3.67, \quad K\Lambda^5 = -9.29; \quad (7)$$

$$\hat{m} \equiv \frac{m_u + m_d}{2} = 5.5 \text{ MeV}, \quad m_s = 135.7 \text{ MeV}. \quad (8)$$

To investigate regimes different than the real one, with a varying number of N_f massless flavors, we will treat quark masses as free parameters, by keeping coupling and cutoff scale fixed as in Eq. (7).

In the following, it will turn out to be more convenient to introduce the following linear combinations of chemical potentials:

$$\mu_q = (\mu_u + \mu_d)/2, \quad \mu_l = (\mu_u - \mu_d)/2. \quad (9)$$

The quark chemical potential μ_q is just one third of the baryon chemical potential $\mu_q = \mu_B/3$. Following the analyses previously performed within the chiral Lagrangian approach [13,14], and NJL [17,23] and ladder-QCD [18] studies, we expect a superfluid phase with condensed pions when the isospin chemical potential μ_l exceeds a critical value μ_l^C ($\mu_l^C = m_\pi/2$ at $\mu_q = T = 0$).

III. BEHAVIOR OF CRITICAL LINES

A. Critical temperature dependence on baryon/isospin chemical potentials

The aim of this section is to shed some light on the physics of QCD at finite baryon chemical potential ($\mu_q = \mu_B/3$), by comparing the physics at $\mu_q \neq 0$ and $\mu_l = 0$ with that at $\mu_q = 0$ and $\mu_l \neq 0$. In fact, the latter case can be studied on the lattice by means of standard importance sampling techniques. The connection of these two regimes could give a deeper understanding of the sign problem in the fermion determinant, and provide us with some procedure to check present simulations and possibly improve numerical algorithms. Rigorous QCD inequalities at non-zero chemical potential have been proposed to try to resolve this question in [24]; the enigma why, at $T = 0$, there exists a critical value for chemical potentials below which the system lies in its ground state has been called ‘‘silver blaze problem.’’ A possible solution of this problem, by using $1/N_c$ expansion, has been proposed in [25,26]. A recent study of phase quenched QCD (a theory where the absolute value of the fermion determinant is taken) has been performed in [27]. We will consider here the dependence of the critical temperatures $T_c(\mu_q) \equiv T_c(\mu_q; \mu_l = 0)$ and $T_c(\mu_l) \equiv T_c(\mu_l; \mu_q = 0)$, for low chemical potentials, obtained by a mean-field analysis of the NJL model. Obviously, mesons and baryons (and diquarks) carry dif-

ferent spin and charges, and their properties depend differently on μ_q and μ_I ; for these reasons, one could expect the two curves $T_c(\mu_q)$ and $T_c(\mu_I)$, when starting by the same value at $\mu_q = \mu_I = 0$, to be different, at least in the regime where bound states heavily influence the thermodynamics of the system. On the other hand, when the free-energy is mainly ruled by the constituent quarks, there is no reason to expect a dependence of the critical curve on the signs of chemical potentials (which will fix the sign of the total charges associated with the system). Here at the mean-field level, the effect of bound states is considered when we admit the formation of a pion condensate. Actually, in agreement with chiral models analyses, in the NJL model the pion effective mass dependence on chemical potentials can be analytically computed [23]; the result is that the charged pions chemical potential is exactly the double of the isospin chemical potential. For this reason, as μ_I is higher than some critical value ($m_\pi/2$ at $T = 0$), a pion condensate starts to form; a similar effect happens when μ_q is higher than the critical value for diquark condensation, which is expected to occur at values $\mu_q > 300 \div 400$ MeV (of course, before diquark condensation, for $\mu_q \sim m_N/3$ and low temperatures there should be the liquid-gas transition for the nucleons). Since in this paper we are interested mainly in the regime of relatively small chemical potentials (lower than ~ 200 MeV) we will neglect the latter possibility. In fact, when the pion condensate is zero, the mean-field effective potential is symmetric under $\mu_u \rightarrow -\mu_u, \mu_d \rightarrow -\mu_d$; this implies that $\mu_q \leftrightarrow \pm \mu_I$ is a symmetry of the problem. Therefore, for zero ρ , the two curves $T_c(\mu_q)$ and $T_c(\mu_I)$ have the same analytical dependence. In Fig. 1 and 2 the phase diagrams in (μ_q, T) , (μ_I, T) spaces are shown; starting from the common value $T_0 = 201$ MeV, corresponding to $\mu_q = \mu_I = 0$, the crossover curves coincide up to the value of about 150 MeV for both chemical potentials. For higher μ_I (and temperatures lower than ~ 200 MeV) we are in the

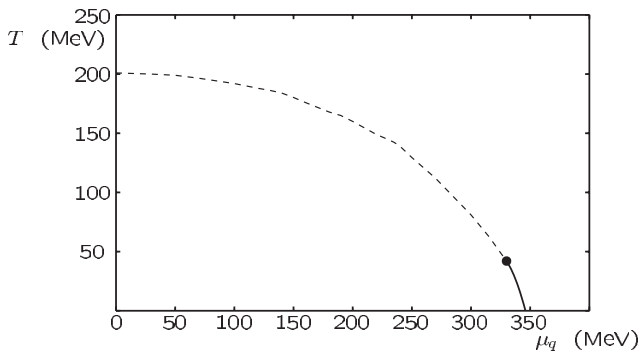


FIG. 1. Phase diagram in the plane (μ_q, T) , for the physical $2 + 1$ case; μ_I and μ_s are set to zero. Dashed/solid lines indicate crossover/first order transitions; consequently, the dot in the picture labels the critical ending point.

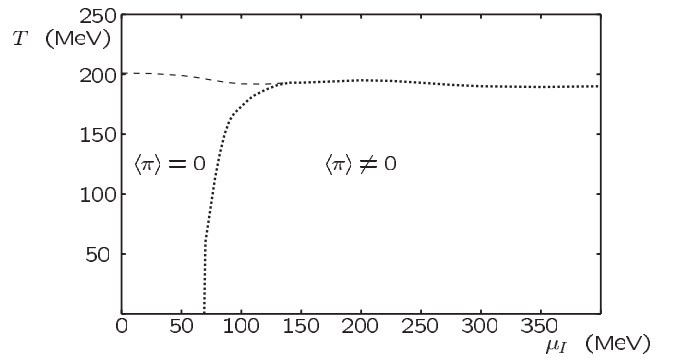


FIG. 2. Phase diagram in the plane (μ_I, T) , for the physical $2 + 1$ case; μ_q and μ_s are set to zero. The dashed line indicates a crossover transition for the scalar condensates, whereas the dotted line stands for genuine second order transition for the pion condensate. In the regions of a nonvanishing pion condensate, the discontinuous behavior of the scalar condensate turns into a continuous one, therefore the critical ending point is not present in this case.

condensed pions phase; in agreement with [23] this regime will persist until $\mu_I \sim 860$ MeV, before the saturation regime takes place. On the other hand, if we follow the crossover line $T_c(\mu_q)$, we will find, as expected, a critical ending point for $\mu_q = 330$ MeV, $T = 42$ MeV and a line of first order transitions for higher μ_q . Summarizing, at this level of calculation (mean field), until isospin chemical potential is lower than the critical value for pion condensation the curves $T_c(\mu_q)$ and $T_c(\mu_I)$ have the same analytical expression $T_c(\mu_q) = T_c(\mu_I)$. This could be interesting in the attempt to extend lattice results from $\mu_I \neq 0$ and $\mu_q = 0$ to $\mu_q \neq 0$ and $\mu_I = 0$ (at least in the region of low chemical potentials). Our conclusions appear to be in agreement with the authors of Ref. [28] (both from the lattice and from a hadron resonances gas model).

B. Order of the transition by varying m_s

It is generally assumed from universality arguments [29] and lattice analyses [30], that the order of the phase transition by increasing temperature at zero density can change as the quark mass values are varied. If in the realistic case (with physical quark masses) the zero density transition is expected to be a crossover, lattice analyses seem to show a first order transition when the three light quark masses are small enough. In particular, by taking $m_u = m_d = 0$, there should be a critical value for m_s below which the transition turns into a discontinuous one: different lattice approaches find m_s^C to be half of the physical value of the strange quark mass [31] or $m_s^C \sim 5 \div 10 m_{u,d}(\text{physical})$ [30]. To study this aspect in the NJL model, we start from the parameters fit of [22], and we take the quark masses as free parameters; namely, we take the four and six fermion couplings fixed so

as to reproduce the phenomenology of the realistical physical situation. This way of proceeding could seem as rather arbitrary, but for any value of the masses considered here, we have verified that the output parameters have reasonable values (critical temperatures $130 \div 200$ MeV, light quark scalar condensates $(-250 \div -240 \text{ MeV})^3$, constituent light quark masses $250 \div 350$ MeV). Of course our results will be strongly model dependent, both for the choice of a specific set of parameters and of a particular model in itself. For instance, the NJL model provides an estimate of the position of the critical point at lower temperatures and higher chemical potentials with respect to those obtained in ladder-QCD and the ones from recent lattice simulation [5]. In Fig. 3 we show the behavior of the light quark scalar condensates vs temperature, in the $m_u = m_d = 0$ limit, and for vanishing chemical potentials too. In the upper picture, m_s is taken to be zero, and for a temperature of about 130 MeV there is a sharp first order transition. As we increase m_s the discontinuity of the scalar condensates reduces (in the lower picture the case $m_s = 8$ MeV is shown), and when m_s exceeds the critical value $m_s^C = 10$ MeV, the zero temperature transition turns into a genuine second order transition. The value we get for m_s^C is in any case smaller than the one from lattice predictions. In Fig. 4 we plot the phase diagram in the (μ_q, m_s) space, by taking $m_u = m_d$ fixed to zero, and $\mu_l = \mu_s = 0$. The label *I/II* indicates, for every couple (μ_q, m_s) , whether, by

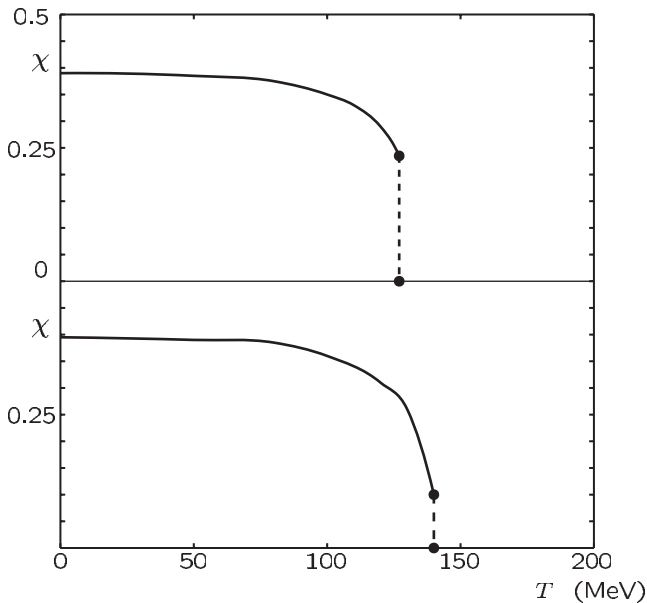


FIG. 3. Behavior of the light quark scalar condensates as a function of temperature at zero chemical potentials and $m_u = m_d = 0$ (upper picture) and $m_s = 8$ MeV (lower picture). In the upper picture, $\chi \equiv \chi_u = \chi_d = \chi_s$, in the lower $\chi \equiv \chi_u = \chi_d$. When the strange quark mass exceeds the critical value $m_s^C = 10$ MeV, the discontinuous behavior turns into a genuine phase transition.

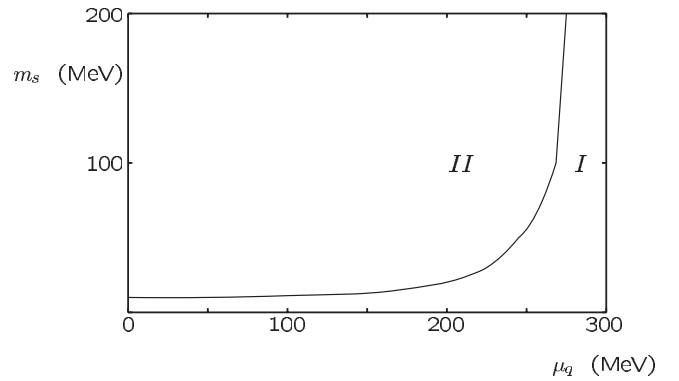


FIG. 4. Phase diagram in the (μ_q, m_s) space, at $m_u = m_d = 0$ and $\mu_l = \mu_s = 0$. For every region in the diagram, the label *I/II* means whether, by increasing temperature and starting from $T = 0$, the transition is of first or second order. Actually, the line in the diagram separating the two different regions follows the critical point by varying m_s .

increasing the temperature starting from zero, the transition is a first or a second order one. Actually, up to $m_s < m_s^C = 10$ MeV, we have first order transition for every value of μ_q , and consequently there is no critical point; for m_s slight above the critical value, the critical point locates at a value of $\mu_q \sim 200$ MeV. The critical value for μ_q grows together with m_s until the strange quark decouples from the two light quarks and the critical point μ_q coordinate is independent on m_s , and lies at $\mu_q \sim 300$ MeV. Finally we have studied whether, in agreement with lattice analyses, a first order transition persists when we consider a nonzero but small $m_u = m_d$: this does not happen in the NJL model with our choice of parameters, for any value of m_s . A recent work based on the linear sigma model had found the critical value for $m_u = m_d = m_s$ to be $m_{\text{crit}} = 40 \pm 20$ MeV [32].

C. Critical lines as a function of N_f

Even though lattice analyses at finite density still present ambiguities in their different approaches, some general features about the critical line appear to be rather solid. In particular, if T_0 is the critical temperature for zero chemical potentials, the dependence of (T/T_0) as a function of (μ/T_0) should be parabolic, (at least in the regime $(\mu/T_0) < 1$), i.e. of the form $(T/T_0) = 1 - \alpha(\mu/T_0)^2$. Secondly, the α coefficient should depend on the number of flavors N_f , increasing with N_f ; in fact, the curves relative to $N_f = 2, 2 + 1, 3$ should be very close to each other and the one relative to $N_f = 4$ should be steeper. It is clear that a dependence of the α coefficient on N_f must be related in any case with a coupling between the flavors; otherwise, the effective potential would become a sum of single flavors contributions, and the critical temperature would not depend on N_f . This fact can give us an idea

about the strength of the coupling between the flavors at the phase transition, and of its possible reduction with temperature. We will check the issue relative to the cases 2, 2 + 1, 3 in the framework of the NJL model. In this context, the aforementioned situations labeled by 2, 3 are those with 2, 3 massless flavors (in the case 2, m_s is set to 5 GeV to decouple the strange quark); 2 + 1 is the physical case with realistic values of quark masses. In the following, μ will indicate a common value for the chemical potential equal for all the active flavors.

In Fig. 5 we show the phase diagrams relative to the cases 2 + 1, 2, 3. Obviously, in case 2, we are in the situation where $m_s < m_s^C$ and we have only first order transitions. As we are varying the quark masses to consider different situations, T_0 has a large range of variation (from 130 to 200 MeV); it is impressive that, as we plot the phase diagrams in dimensionless units, those large differences cancel out almost completely. This is the most striking evidence that our approach, in its simplicity, has some validity.

2	$\alpha = 0.0507 \pm 0.0034;$	$\mu_u = \mu_d = \mu$	[6]	
2	$\alpha = 0.0504 \pm 0.0036;$	$\mu_u = \mu_d = \mu$	[8]	
2	$\alpha = 0.07 \pm 0.03;$	$\mu_u = \mu_d = \mu$	[10]	
2 + 1	$\alpha = 0.0288 \pm 0.0009;$	$\mu_u = \mu_d = \mu_s = \mu = \mu_B/3$	[4]	(11)
3	$\alpha = 0.0610 \pm 0.0009;$	$\mu_u = \mu_d = \mu_s = \mu = \mu_B/3$	[8]	
3	$\alpha = 0.114 \pm 0.046;$	$\mu_s = 0$	[10]	
4	$\alpha = 0.099;$	$\mu_f = \mu = \mu_B/3$	[6].	

We find that our predictions for α are bigger than those obtained by lattice approaches, apart from [10] for $N_f = 3$; in that case, the results are comparable. A recent study based on a hadron resonance gas model [28] give the result

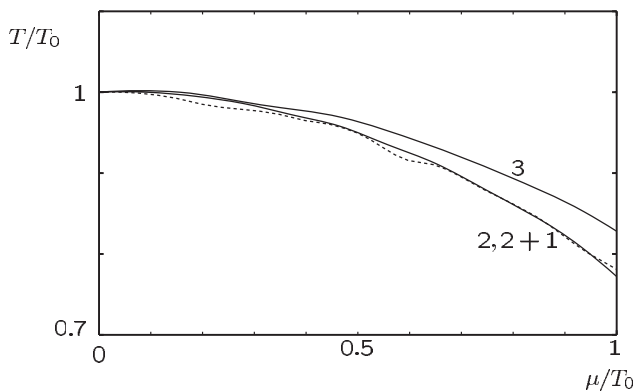


FIG. 5. Plot of the three cases 2, 2 + 1, 3 in dimensionless units ($\mu/T_0, T/T_0$), $\mu/T_0 \leq 1$. The curves relative to 2 and 2 + 1 (the dashed one) almost overlap. In disagreement with lattice simulations, the curve relative to 3 stands slight above the others.

When showing the three cases on the same diagram, we can clearly observe the surprising overlap of the results. The agreement between 2 and 2 + 1 cases (apart from numerical instabilities related with 2 + 1 case) is remarkable, and good between 2 and 3 cases; the slope of case 3, with respect to the lattice previsions, is smaller than that of 2, but the difference is slight.

The results we get for α are the following:

$$\begin{aligned}
 2 & \quad \alpha = 0.1995 \pm 0.025, \\
 2 + 1 & \quad \alpha = 0.2496 \pm 0.0623, \\
 3 & \quad \alpha = 0.1614 \pm 0.011.
 \end{aligned} \tag{10}$$

The worse precision we obtain for the 2 + 1 case depends on the larger error in the determination of the cross-over curve.

For completeness, we quote the results for α from lattice analyses:

$\alpha = 0.17 \pm 0.01$ and this value is in a good agreement with our results. A study within a chiral quark model give for α a value of about 0.1, extracted from Fig. 2 of [33].

We have also studied the behavior of the critical curve in ladder-QCD [34] (in its version [18]); in this model there is no coupling between flavors, therefore it is independent on N_f . We have found that the critical curve is flatter than that of NJL model, namely, the coefficient α is much smaller, and hence closer to lattice predictions: $\alpha = 0.0797 \pm 0.0056$. We have attributed this feature to the lack of coupling between flavors in the model. On the other hand, since the value for the α coefficient we find in the NJL model is slightly higher than the value found in Ref. [28] and sensibly higher than the values obtained from other lattice analyses, we can argue that introducing an effective reduction of the K coupling with temperature, as considered in Ref. [22,35], α would decrease at the meantime. Therefore, by considering the following temperature dependence of the 't Hooft term

$$K(T) = K_0 \exp(-T/T_1)^2, \tag{12}$$

we have verified that reducing T_1 the critical temperature at $\mu = 0$ is also reduced; in this way, the curve gets

flatter. By taking two different values for T_1 , and considering for simplicity the case 2, we find the value $\alpha = 0.1186 \pm 0.0061$ in the case $T_1 = 160$ MeV, and $\alpha = 0.1084 \pm 0.0035$ in the case $T_1 = 100$ MeV. In this way, the agreement with lattice is considerably improved; this can be considered an indirect proof of $U(1)_A$ effective restoration with temperature.

For the sake of completeness, we have also studied the two flavor NJL model with the 't Hooft determinant. The model is not completely equivalent to the three flavor model in the limit of infinite m_s , since in the latter case a strange quark loop gives a contribution, proportional to the strange quark condensate, to the light quark constituent mass. In any case we do not expect a dramatic change in our results, with respect to previous expectations, for the behavior of the critical curve. We consider in this case the following expression for the interaction part of the Lagrangian (the $U(1)_A$ breaking determinant term can be rewritten as a four-fermion interaction):

$$\begin{aligned} \mathcal{L}_{\text{int}} = & G_1[(\bar{q}q)^2 + (\bar{q} \vec{\tau} q)^2 + (\bar{q}i\gamma_5 q)^2 + (\bar{q}i\gamma_5 \vec{\tau} q)^2] \\ & + G_2[(\bar{q}q)^2 - (\bar{q} \vec{\tau} q)^2 - (\bar{q}i\gamma_5 q)^2 + (\bar{q}i\gamma_5 \vec{\tau} q)^2] \end{aligned} \quad (13)$$

with

$$G_1 = (1 - \beta)G_0; \quad G_2 = \beta G_0. \quad (14)$$

The β coefficient tells us how hard the flavor mixing is; it is maximal for $G_1 = 0$, namely, for $\beta = 1$.

For the choice of the parameters G_1 and G_2 we follow the approach proposed in Ref. [20,22]. In Ref. [22] the authors study the original two flavor Lagrangian, proposed by Nambu and Jona-Lasinio, with $G_1 = G_2$ and therefore $\beta = 0.5$. The value we find in this case for α is very similar with the result we obtained in the $SU(3)$ case in the limit $m_s \rightarrow \infty$:

$$\alpha = 0.2107 \pm 0.0214. \quad (15)$$

The authors of Ref. [20] take β as a free parameter instead. Here we furthermore consider the possible dependence of G_2 coefficient on the temperature, $G_2 = G_2(T = 0) \exp(-(T/T_1)^2)$.

If we take G_2 independent on the temperature (namely with $T_1 = \infty$), the value we find for the α coefficient does

not change by varying β :

$$\alpha = 0.2142 \pm 0.0259 \quad (16)$$

again in agreement with previous analyses. On the other hand, if we admit a restoration of $U(1)_A$ symmetry with temperature, we find a dependence on the β coefficient. For $\beta = 0.2$ we have

$$\alpha = 0.1484 \pm 0.009 \quad \text{for } T_1 = 160 \text{ MeV} \quad (17)$$

and

$$\alpha = 0.1196 \pm 0.0161 \quad \text{for } T_1 = 100 \text{ MeV}. \quad (18)$$

For $\beta = 0.3$ we have

$$\alpha = 0.1024 \pm 0.0042 \quad \text{for } T_1 = 160 \text{ MeV} \quad (19)$$

and

$$\alpha = 0.08101 \pm 0.007 \quad \text{for } T_1 = 100 \text{ MeV}. \quad (21)$$

However, according to Shuryak [36] it is very unlikely that restoration of $U(1)_A$ can occur before chiral symmetry restoration; therefore, the value $T_1 = 100$ MeV should not be taken too seriously. In any case, it appears clear that restoration of $U(1)_A$ symmetry can strongly influence the behavior of the critical curve.

IV. CONCLUSIONS

In this paper we have studied some general features of the QCD critical line in the framework of a NJL model. In section one, we have compared the physics at $\mu_q \neq 0$ with that at $\mu_l \neq 0$. In section two, we have varied quark masses to show that the order of finite temperature transition changes if we consider small enough masses. In section three, we have studied the dependence of the slope of the critical curve T_c vs μ on N_f . In recent times these questions have received much attention from the lattice community, due to the great improvement of finite chemical potential algorithms of simulation.

ACKNOWLEDGMENTS

We wish to thank M. P. Lombardo and D. Toublan for useful discussions.

[1] M. Asakawa and K. Yazaki, Nucl. Phys. **A504**, 668 (1989); A. Barducci, R. Casalbuoni, S. De Curtis, R. Gatto, and G. Pettini, Phys. Lett. B **231**, 463 (1989); Phys. Rev. D **41**, 1610 (1990); A. Barducci, R. Casalbuoni, G. Pettini, and R. Gatto, Phys. Rev. D **49**, 426 (1994).

[2] M. A. Halasz, A. D. Jackson, R. E. Shrock, M. A. Stephanov, and J. J. M. Verbaarschot, Phys. Rev. D **58**, 096007 (1998).

[3] K. Rajagopal and F. Wilczek, hep-ph/0011333; O. Scavenius, A. Mocsy, I. N. Mishustin, and D. H. Rischke, Phys. Rev. C **64**, 045202 (2001).

- [4] Z. Fodor and S. D. Katz, *J. High Energy Phys.* **03** (2002) 014.
- [5] Z. Fodor and S. D. Katz, *J. High Energy Phys.* **04** (2004) 050.
- [6] M. D’Elia and M. P. Lombardo, *Phys. Rev. D* **67**, 014505 (2003).
- [7] P. de Forcrand and O. Philipsen, *Nucl. Phys.* **B642**, 290 (2002).
- [8] P. de Forcrand and O. Philipsen, *Nucl. Phys.* **B673**, 170 (2003).
- [9] C. R. Allton *et al.*, *Phys. Rev. D* **66**, 074507 (2002).
- [10] S. Ejiri, C. R. Allton, S. J. Hands, O. Kaczmarek, F. Karsch, E. Laermann, and C. Schmidt, *Prog. Theor. Phys. Suppl.* **153**, 118 (2004).
- [11] J. B. Kogut and D. K. Sinclair, *Phys. Rev. D* **66**, 034505 (2002).
- [12] S. Gupta, hep-lat/0202005.
- [13] D. T. Son and M. A. Stephanov, *Phys. Rev. Lett.* **86**, 592 (2001).
- [14] M. Loewe and C. Villavicencio, *Phys. Rev. D* **67**, 074034 (2003).
- [15] B. Klein, D. Toublan, and J. J. M. Verbaarschot, *Phys. Rev. D* **68**, 014009 (2003).
- [16] D. Toublan and J. B. Kogut, *Phys. Lett. B* **564**, 212 (2003).
- [17] A. Barducci, R. Casalbuoni, G. Pettini, and L. Ravagli, *Phys. Rev. D* **69**, 096004 (2004).
- [18] A. Barducci, G. Pettini, L. Ravagli, and R. Casalbuoni, *Phys. Lett. B* **564**, 217 (2003).
- [19] A. Barducci, R. Casalbuoni, G. Pettini, and L. Ravagli, *Phys. Rev. D* **71**, 016011 (2005).
- [20] M. Frank, M. Buballa, and M. Oertel, *Phys. Lett. B* **562**, 221 (2003).
- [21] S. P. Klevansky, *Rev. Mod. Phys.* **64**, 649 (1992).
- [22] T. Hatsuda and T. Kunihiro, *Phys. Rep.* **247**, 221 (1994); T. Maruyama, K. Tsushima, and A. Faessler, *Nucl. Phys. A* **537**, 303 (1992).
- [23] L. Y. He, M. Jin, and P. F. Zhuang, *Phys. Rev. D* **71**, 116001 (2005).
- [24] T. D. Cohen, hep-ph/0405043.
- [25] T. D. Cohen, *Phys. Rev. D* **70**, 116009 (2004).
- [26] D. Toublan, *Phys. Lett. B* **621**, 145 (2005).
- [27] K. Splittorff, hep-lat/0505001.
- [28] D. Toublan and J. B. Kogut, *Phys. Lett. B* **605**, 129 (2005).
- [29] R. D. Pisarski and F. Wilczek, *Phys. Rev. D* **29**, 338 (1984).
- [30] E. Laermann and O. Philipsen, *Annu. Rev. Nucl. Part. Sci.* **53**, 163 (2003).
- [31] F. R. Brown *et al.*, *Phys. Rev. Lett.* **65**, 2491 (1990); S. Aoki *et al.* (JLQCD Collaboration), *Nucl. Phys. B Proc. Suppl.* **73**, 459 (1999).
- [32] T. Herpay, A. Patkos, Z. Szep, and P. Szepfalusy, *Phys. Rev. D* **71**, 125017 (2005).
- [33] A. Jakovac, A. Patkos, Z. Szep, and P. Szepfalusy, *Phys. Lett. B* **582**, 179 (2004).
- [34] A. Barducci, R. Casalbuoni, S. De Curtis, D. Dominici, and R. Gatto, *Phys. Rev. D* **38**, 238 (1988).
- [35] P. Costa, M. C. Ruivo, C. A. de Sousa, and Y. L. Kalinovsky, *Phys. Rev. D* **71**, 116002 (2005).
- [36] E. V. Shuryak, *Comments Nucl. Part. Phys.* **21**, 235 (1994).